9
Multi-Regge theory

9.1 Introduction

So far we have limited our attention to four-particle scattering amplitudes (i.e. to processes of the form $1+2\to 3+4$). These have the advantage of being kinematically rather similar to the potential-scattering amplitudes, for which the basic ideas of Regge theory were originally developed. In particular they depend on only two independent variables, s and t, and so it is a fairly straightforward matter to make analytic continuations in J and t. Also there is a wealth of two-body-final-state data with which to compare the predictions of the theory.

Though the initial state of any physical scattering process will always in practice be a two-particle state (counting bound states such as deuterons as single particles), except at very low energies particle production is always likely to occur. And as the energy increases two-body and quasi-two-body final states make up a diminishing fraction of all the events. So it is very desirable to be able to extend our understanding of Regge theory so as to obtain predictions for many-body final states. Theoretically, this is even more necessary, since models like fig. 3.3 for Regge poles or fig. 8.6 for Regge cuts demonstrate how even in $2\to 2$ amplitudes Regge theory makes essential use of many-body unitarity. So if we are to have any hope of making Regge theory self-consistent (in the bootstrap sense, for example) we must be able to describe such intermediate states in terms of Regge singularities.

In principle this is a fairly simple matter since if we consider for example the amplitude fig. 9.1 (a) with s_{12}, s_{34}, $s_{45}\to\infty$ we may expect from fig. 9.1 (b) that

$$A \sim (s_{34})^{\alpha_1(t_1)}(s_{45})^{\alpha_2(t_2)}\beta(t_1, t_2, s_{12}, s_{34}, s_{45}) \qquad (9.1.1)$$

and indeed this is so. However, there are several problems to be solved before we can be sure that this result is right. It is necessary to understand how to define scattering angles, and thence partial-wave amplitudes, for many-body processes, and how to continue them analytically both in J and in the channel invariants. We must also be clear about

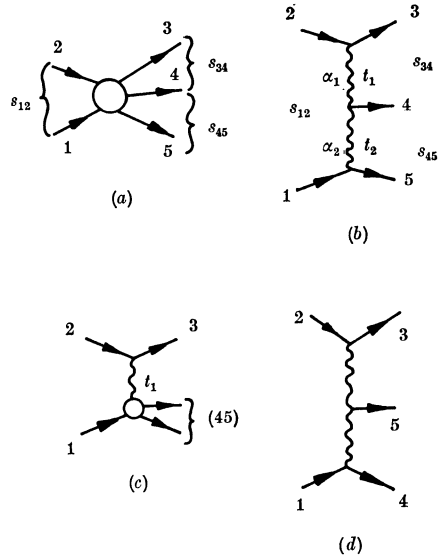

FIG. 9.1 (*a*) The amplitude for $1+2\to3+4+5$. (*b*) A double-Regge model for this process. (*c*) $1+2\to3+(45)$. (*d*) Another double-Regge coupling.

which variables are being kept fixed and which tend to infinity when we take a given Regge limit, the singularity structure of the amplitude in these variables, and the order in which the limits are to be taken. And the central vertex in fig. 9.1 (*b*) involves Reggeons whose spin and helicity depend on α so we must check on the resulting kinematical factors.

In fact most of these questions cannot yet be tackled rigorously because to do so would require a more detailed understanding of the singularity structure of many-particle amplitudes than has so far been achieved. Hence we shall adopt a rather simple-minded approach, and assume that the methods which we adopted in chapters 1 and 2 can be extended in the most obvious way without mishap. A more thorough account of present theoretical knowledge can be found in Brower, de Tar and Weis (1974).

In the next section we review the kinematics of many-body processes, and we then go on to consider the different Regge asymptotic limits which may be taken. This is followed by a more detailed discussion of the $2\to3$ amplitude, on the basis of which we postulate some general rules for any multi-Regge amplitudes. It is rather remarkable that the dual models of chapter 7 can readily be extended to many-body amplitudes, and as they provide a good deal of insight into the

nature of multi-Regge couplings we outline the main results. The chapter concludes with a very short discussion of some phenomenological applications of the theory.

9.2 Many-particle kinematics

We consider first the process $1+2\to 3+4+5$ shown in fig. 9.1. For simplicity we suppose that all the external particles are spinless.

The square of the centre-of-mass energy is (cf. (1.7.5))

$$s \equiv s_{12} = (p_1+p_2)^2 = (p_3+p_4+p_5)^2 \equiv s_{345} \tag{9.2.1}$$

Similarly, for the outgoing two-body channels we have the subenergies

$$s_{34} = (p_3+p_4)^2, \quad s_{45} = (p_4+p_5)^2 \quad \text{and} \quad s_{35} = (p_3+p_5)^2 \tag{9.2.2}$$

The 6 crossed-channel invariants, involving both incoming and outgoing particles are,

$$\left.\begin{aligned} t_1 \equiv t_{23} &= (p_2-p_3)^2, \quad t_{24} = (p_2-p_4)^2, \quad t_{25} = (p_2-p_5)^2 \\ t_2 \equiv t_{15} &= (p_1-p_5)^2, \quad t_{14} = (p_1-p_4)^2, \quad t_{13} = (p_1-p_3)^2 \end{aligned}\right\} \tag{9.2.3}$$

Clearly any three-particle invariant will be equal to some two-particle invariant (as in (9.2.1)) because of four-momentum conservation, so the 10 variables defined in (9.2.1), (9.2.2) and (9.2.3) include all the independent invariants. But evidently they cannot all be independent because we showed in section 1.4 than an n-line amplitude has only $3n-10$ independent variables, so with $n=5$ only 5 can be regarded as independent variables. In the centre-of-mass frame of particles 4 and 5, i.e. where $\boldsymbol{q}_4+\boldsymbol{q}_5=\mathbf{0}$, s_{45} is the square of the total energy of these particles, i.e.

$$s_{45} \equiv (p_4+p_5)^2 = (E_4+E_5, \mathbf{0})^2 = (E_4+E_5)^2 = m_{45}^2 \tag{9.2.4}$$

and m_{45} is called the 'invariant mass' of the 'quasi-particle' (45). So if we regard the reaction of fig. 9.1 (a) as the process $1+2\to 3+(45)$ shown in fig. 9.1 (c) we have, like (1.7.21),

$$s_{12}+t_{23}+t_{13} = m_1^2+m_2^2+m_3^2+s_{45} \equiv \Sigma_{45} \tag{9.2.5}$$

with similar relations for other pairings of particles.

A convenient choice of independent invariants suggested by fig. 9.1 (b) is

$$s_{12}, s_{34}, s_{45}, t_1 \text{ and } t_2, \tag{9.2.6}$$

but this depends on how we choose to couple the particles together, and fig. 9.1 (d) for example, suggests a quite different choice.

https://doi.org/10.1017/9781009403269.010 Published online by Cambridge University Press

In the centre-of-mass frame $q_1 + q_2 = 0$ the energies and momenta of particles 1 and 2 are given by (1.7.8), (1.7.9) and (1.7.10), i.e.

$$E_1 = \frac{1}{2\sqrt{s}}(s + m_1^2 - m_2^2), \quad q_{s12}^2 = \frac{1}{4s}\lambda(s, m_1^2, m_2^2) \tag{9.2.7}$$

etc. Similarly if we regard (45) as a single particle of mass $m_{45} = \sqrt{s_{45}}$ as above, it is clear that in this frame

$$E_3 = \frac{1}{2\sqrt{s}}(s + m_3^2 - s_{45}), \quad q_{s3}^2 = \frac{1}{4s}\lambda(s, m_3^2, s_{45}) \tag{9.2.8}$$

with similar expressions for particles 4 and 5.

Also the scattering angle between the direction of motion of particle 3 and that of particle 2 is given by (1.7.17) with $\sqrt{s_{45}}$ instead of m_4, i.e.

$$z_{23} = \cos\theta_{s23} = \frac{s^2 + s(2t_1 - \Sigma_{45}) + (m_1^2 - m_2^2)(m_3^2 - s_{45})}{\lambda^{\frac{1}{2}}(s, m_1^2, m_2^2)\,\lambda^{\frac{1}{2}}(s, m_3^2, s_{45})} \tag{9.2.9}$$

and the physical region for this scattering process is given by (1.7.24) with the obvious substitutions.

The four-momentum conservation relation (9.2.1)

$$s_{12} = (p_3 + p_4 + p_5)^2$$

with (9.2.2) and (1.7.4) gives

$$s_{12} = s_{34} + s_{45} + s_{35} - m_3^2 - m_4^2 - m_5^2 \tag{9.2.10}$$

so for a given fixed s_{12} only two of the three sub-energies are independent, and the boundary of the physical region, determined by (1.7.24) with the substitutions described above, is as shown in fig. 9.2. This is known as a Dalitz plot (Dalitz 1953). If there is a resonance, r, which decays into particles $(4+5)$, as in fig. 9.3, we can expect that for a given fixed s_{12} there will be a peak in the cross-section as a function of s_{45} along the line $s_{45} = M_r^2$. Likewise if 3 and 4 resonate there will be a peak at fixed s_{34}, while if 3 and 5 resonate there will be a diagonal line across the plot at fixed s_{35}. So a plot like fig. 9.2 is very useful for deciding which pairs of particles, if any, are resonating.

But our main interest lies in examining Regge exchanges like fig. 9.1 (*b*), and for this purpose we need to be able to define angular momenta for the various t channels. Thus one of the crossed processes to fig. 9.1 is fig. 9.4 (*a*), i.e.

$$2 + \bar{3} \to (\bar{1}5) + 4 \tag{9.2.11}$$

where we treat $\bar{1}5$ as a quasi-particle of mass $(p_1 - p_5)^2 = t_2$. The centre-of-mass energies and momenta can all be obtained from

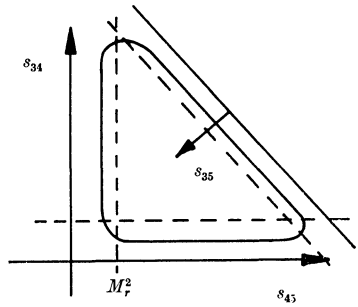

FIG. 9.2 Dalitz plot of the variation of s_{34}, s_{45} and s_{35} for a given s_{12} constrained by (9.2.10). The boundary of the physical region determined by (1.7.24) with the obvious substitutions is shown. The dotted lines mark positions where resonance peaks may occur.

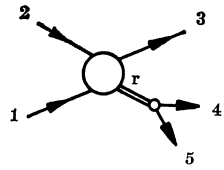

FIG. 9.3 The amplitude for $1+2 \to 3+\mathrm{r}$, $\mathrm{r} \to 4+5$.

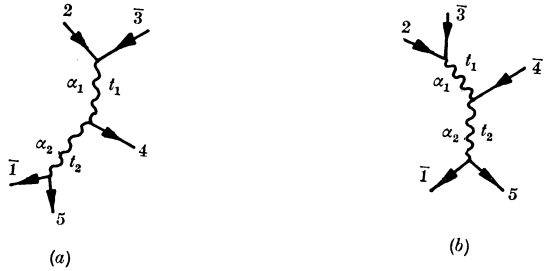

FIG. 9.4 (*a*) The crossed-channel process $2+\bar{3} \to (\bar{1}5)+4$.
(*b*) The crossed-channel process $(2\bar{3})+\bar{4} \to \bar{1}+5$.

(1.7.15) with the obvious substitutions, where now $t \to t_{23} \equiv t_1$, and the centre-of-mass scattering angle of particle 4 with respect to the direction of $\bar{3}$ is given by (1.7.19), viz.

$$\cos\theta_{34} \equiv z_{t34} \equiv z_1 = \frac{t_1^2 + t_1(2s_{34} - \Sigma_{15}) + (m_2^2 - m_3^2)(t_2 - m_4^2)}{\lambda^{\frac{1}{2}}(t_1, m_2^2, m_3^2)\,\lambda^{\frac{1}{2}}(t_1, t_2, m_4^2)}$$

where
$$\Sigma_{15} \equiv m_2^2 + m_3^2 + m_4^2 + t_2 \qquad (9.2.12)$$

This is the scattering angle in the centre-of-mass system of $2+\bar{3}$, i.e $\boldsymbol{q}_2 + \boldsymbol{q}_3 = 0$. But the process (9.2.11) differs from a $2 \to 2$ spinless-

https://doi.org/10.1017/9781009403269.010 Published online by Cambridge University Press

particle scattering process not only because of the variation of the 'mass' of the $(\bar{1}5)$ system, but also because the $(\bar{1}5)$ quasi-particle carries angular momentum. It will subsequently 'decay' into the particles $\bar{1}$ and $\bar{5}$ with an angular distribution which depends on the helicity of $(\bar{1}5)$ in the 2–$\bar{3}$ centre-of-mass system (like (4.2.13)).

Then for the process

$$(2\bar{3}) + \bar{4} \to \bar{1} + 5 \tag{9.2.13}$$

(fig. 9.4(*b*)) we proceed to the $\bar{1}$–5 centre-of-mass frame, in which the scattering angle of 5 relative to the direction of $\bar{4}$ is

$$\cos\theta_{45} \equiv z_{t45} \equiv z_2 = \frac{t_2^2 + t_2(2s_{45} - \Sigma_{23}) + (t_1 - m_4^2)(m_1^2 - m_5^2)}{\lambda^{\frac{1}{2}}(t_2, t_1, m_4^2)\,\lambda^{\frac{1}{2}}(t_2, m_1^2, m_5^2)} \tag{9.2.14}$$

The azimuthal angle ω_{12} between the plane containing particles 4 and 5 and that containing 3 and 4 (see fig. 9.5) is called the Toller angle (or helicity angle) (Toller 1968). This angle may be evaluated with some effort (see Chan, Kajantie and Ranft 1967) as follows.

Since ω_{12} is the angle about the direction of particle 4 it will be unaltered if we make a Lorentz boost to the rest frame of particle 4. This makes the kinematics much easier to cope with. In this rest frame the Toller angle is defined by

$$\cos\omega_{12} = \frac{(\boldsymbol{q}_2 \times \boldsymbol{q}_3).(\boldsymbol{q}_1 \times \boldsymbol{q}_5)}{|\boldsymbol{q}_2 \times \boldsymbol{q}_3|\,|\boldsymbol{q}_1 \times \boldsymbol{q}_5|} \tag{9.2.15}$$

i.e. the angle between the plane containing particles 2 and 3 and that containing 1 and 5. Since, from (1.7.2) and (1.7.4),

$$\boldsymbol{q}_i.\boldsymbol{q}_j = E_iE_j - p_i.p_j, \quad \boldsymbol{q}_i^2 = -m_i^2 + E_i^2, \quad i,j = 1,\ldots,5 \tag{9.2.16}$$

in the rest frame of 4, where $\boldsymbol{q}_4 = 0$, $E_4 = m_4$,

$$E_i = \frac{p_i.p_4}{m_4} \tag{9.2.17}$$

But
$$s_{ij} \equiv (p_i + p_j)^2 = p_i^2 + p_j^2 + 2p_i.p_j = m_i^2 + m_j^2 + 2p_i.p_j \tag{9.2.18}$$

so
$$\left.\begin{aligned} E_i &= \frac{1}{2m_4}(s_{i4} - m_i^2 - m_4^2), \quad i = 3,5 \\ &= \frac{1}{2m_4}(t_{i4} - m_i^2 - m_4^2), \quad i = 1,2 \end{aligned}\right\} \tag{9.2.19}$$

Now
$$\begin{aligned} |\boldsymbol{q}_2 \times \boldsymbol{q}_3| &= |\boldsymbol{q}_2|\,|\boldsymbol{q}_3| \sin\theta_{23} \\ &= |\boldsymbol{q}_2|\,|\boldsymbol{q}_3|(1 - \cos^2\theta_{23})^{\frac{1}{2}} = [\boldsymbol{q}_2^2\,\boldsymbol{q}_3^2 - (\boldsymbol{q}_2.\boldsymbol{q}_3)^2]^{\frac{1}{2}} \end{aligned} \tag{9.2.20}$$

https://doi.org/10.1017/9781009403269.010 Published online by Cambridge University Press

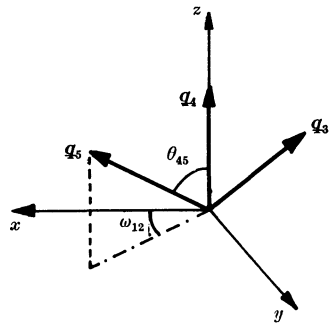

FIG. 9.5 Angles in the $\bar{1}$–5 centre-of-mass system. q_4 is along the z axis, q_3 is in the x–z plane, and ω_{12} is the angle between the plane containing q_3 and q_4 and that containing q_4 and q_5, i.e. between q_5 and the x–z plane.

and Lagrange's identity gives

$$(q_2\times q_3)\cdot(q_1\times q_5)=(q_2\cdot q_1)(q_3\cdot q_5)-(q_2\cdot q_5)(q_3\cdot q_1) \quad (9.2.21)$$

and all these scalar products can be evaluated using (9.2.16). Thus

$$q_2\cdot q_3=E_2E_3-p_2\cdot p_3=\frac{1}{2m_4}(t_{24}-m_2^2-m_4^2)\times\frac{1}{2m_4}(s_{34}-m_3^2-m_4^2)-\frac{t_{23}-m_2^2-m_3^2}{2} \quad (9.2.22)$$

$$\text{so}\qquad (q_2\cdot q_3)^2\to\left(\frac{t_{24}s_{34}}{4m_4^2}\right)^2-\frac{t_{24}s_{34}t_{23}}{4m_4^2}\quad\text{for}\quad t_{24},s_{34},t_{23}\gg m_i^2 \quad (9.2.23)$$

$$\text{And}\qquad q_2^2\,q_3^2=(E_2^2-m_2^2)(E_3^2-m_3^2)\to\frac{s_{34}^2t_{24}^2}{(2m_4)^4} \quad (9.2.24)$$

in the same limit, giving

$$|q_2\times q_3|\to\left(\frac{t_{23}t_{24}s_{34}}{4m_4^2}\right)^{\frac{1}{2}} \quad (9.2.25)$$

But, like (9.2.5), we have

$$t_{24}+t_{23}+s_{34}=m_2^2+m_3^2+m_4^2+t_{15} \quad (9.2.26)$$

$$\text{so that}\qquad t_{24}\to-s_{34},\quad s_{34}\to\infty\quad\text{at fixed}\quad t_{23},t_{15}$$

$$\text{and hence}\qquad |q_2\times q_3|\to\frac{s_{34}}{2m_4}\sqrt{-t_{23}} \quad (9.2.27)$$

$$\text{Similarly}\qquad |q_4\times q_5|\to\frac{s_{45}}{2m_4}\sqrt{-t_{15}} \quad (9.2.28)$$

and with more effort we find

$$(q_2\times q_3)\cdot(q_1\times q_5)\to\frac{1}{8m_4^2}\{s_{12}[(t_{23}+t_{15}-m_4^2)^2-4t_{23}t_{15}]+s_{34}s_{45}(t_{23}+t_{15}-m_4^2)\} \quad (9.2.29)$$

https://doi.org/10.1017/9781009403269.010 Published online by Cambridge University Press

so that from (9.2.15) with $t_1 \equiv t_{23}$, $t_2 \equiv t_{15}$,

$$\cos\omega_{12} \approx \frac{1}{2\sqrt{-t_1}\sqrt{-t_2}}\left(t_1+t_2-m_4^2+\frac{s_{12}}{s_{34}s_{45}}\lambda(t_1,t_2,m_4^2)\right) \tag{9.2.30}$$

in the limit $s_{12}, s_{34}, s_{45} \gg t_1, t_2, m_1^2, \ldots, m_5^2$. At fixed t_1, t_2 it is often more convenient to use the variable η_{12} defined by

$$\eta_{12} \equiv \frac{s_{12}}{s_{34}s_{45}} = \frac{s_{345}}{s_{34}s_{45}} \tag{9.2.31}$$

rather than ω_{12}.

The set of variables $\quad t_1, t_2, z_1, z_2$ and η_{12} (9.2.32)

provide an alternative to (9.2.6), and one which is more useful for Reggeization.

To extend this approach to the six-particle amplitude, fig. 9.6(*a*), we simply note that it becomes similar to the five-particle amplitude, fig. 9.1 if we regard $(1\bar{6})$ as a particle, and replace s_{12} by $s_{345} \equiv (p_3+p_4+p_5)^2$, but in addition to the scattering angles z_1 and z_2 and the Toller variable $\eta_{12} = s_{345}/s_{34}s_{45}$ we also have z_3, the centre-of-mass scattering angle for $(2\bar{3}\bar{4})+5 \to \bar{1}+6$, and the Toller angle ω_{23}, the angle between the plane containing particles 5 and 6 and that containing 4 and 5 in the $\bar{1}$–6 rest frame. Or instead we can use $\eta_{23} \equiv s_{456}/s_{45}s_{56}$. The sets of variables

$$t_1, t_2, t_3, s_{34}, s_{45}, s_{56}, s_{345}, s_{456}, \quad \text{or} \quad t_1, t_2, t_3, z_1, z_2, z_3, \eta_{12}, \eta_{23} \tag{9.2.33}$$

give the required 8 independent variables for a 6-line amplitude. Of course these sets are convenient only if we choose to couple the particles as in fig. 9.6(*a*), rather than, say, fig. 9.6(*b*) for which a different set of angular variables is appropriate (see below).

As the number of external lines increases so does the number of different ways of coupling together the particles. But for any given configuration a complete set of variables is provided by the momentum transfers, t_i, the cosines of the scattering angles, z_i, and the Toller variables, η_{ij}, associated with each adjacent pair of t's (t_i and t_j say). And for given fixed values of the t's these angle variables can all be expressed in terms of the s's.

https://doi.org/10.1017/9781009403269.010 Published online by Cambridge University Press

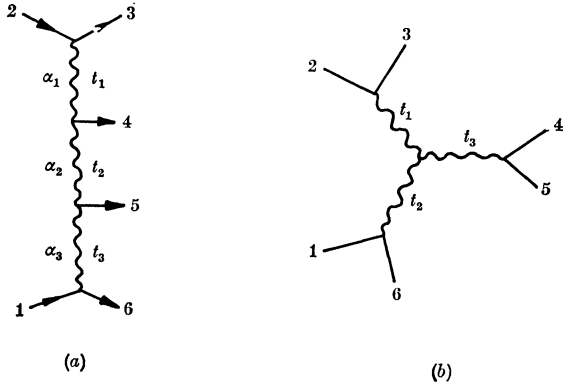

FIG. 9.6 (*a*) Multi-Regge amplitude for $1+2\to 3+4+5+6$.
(*b*) Another multi-Regge coupling.

9.3 Multi-Regge scattering amplitudes

The Froissart–Gribov partial-wave projection (2.5.3), in terms of which Regge poles were defined in $2\to 2$ scattering, involves integration over the s-discontinuity of the scattering amplitude (2.7.2). The pole appears in the power behaviour of this discontinuity. So when generalizing to a multi-Regge limit of a many-particle scattering process we shall have to concern ourselves with simultaneous discontinuities in several variables.

It is obviously essential that these discontinuities should be independent in the asymptotic limit. For normal threshold discontinuities it is easy to decide when they are independent. In an $n\to m$ scattering amplitude, fig. 9.7, we can distinguish between overlapping channels such as x and y, for which the invariants

$$s_x \equiv s_{1,\dots,i} \equiv (p_1+p_2+\dots+p_i)^2$$

and

$$s_y \equiv s_{i-1,i,\dots,j} \equiv (p_{i-1}+p_i+\dots+p_j)^2$$

have the particles i and $i-1$ in common, and non-overlapping channels like s_x and s_z which have no particles in common and are therefore independent. The normal-threshold discontinuity of a given channel is a singularity just in that channel's invariant (e.g. the 12 threshold branch point is at $s_{12}\equiv(p_1+p_2)^2=(m_1+m_2)^2$) and so normal-threshold discontinuities in non-overlapping channels are independent of each other. But more complicated Landau curves do not have this independence. For example the box diagram, fig. 1.10(*b*), gives the s–t curve (1.12.10) for the position of the double discontinuity. It is

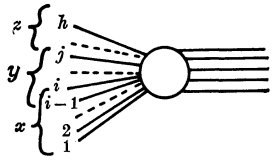

FIG. 9.7 An $n \to m$ amplitude. The invariant $s_x \equiv (p_1+p_2+\ldots+p_i)^2$ overlaps $s_y \equiv (p_{i-1}+p_i+\ldots+p_j)^2$ but not $s_z \equiv (p_j+\ldots+p_n)^2$.

generally assumed that the normal-threshold discontinuities are sufficient to give the Regge asymptotic behaviour, in which case only non-overlapping channels have simultaneous Regge discontinuities. This is trivial in $2\to2$ scattering since we obviously do not have simultaneous Regge behaviour in the overlapping $s \equiv (p_1+p_2)^2$ and $t \equiv (p_1-p_3)^2$ channels, but it has not been established for certain in more complex amplitudes. It is, however, true in all the simple models such as ladder diagrams or dual models and we adopt it here (see Brower *et al.* 1974).

There are generally several different asymptotic limits which can be taken for a given amplitude and for a given configuration of the particles, depending on which variables are taken to infinity, and which are held fixed. Thus in the five-particle amplitude, fig. 9.1, we have the following possibilities.

(*a*) *The single-Regge limit.* In this case $z_1\to\infty$ but t_1 and the other angles and invariants in (9.2.32) are held fixed. This means $s_{34}\to\infty$ from (9.2.12), and hence $s_{12}\to\infty$ from (9.2.10) but s_{45}, t_1 and t_2 are fixed. Also to keep ω_{12} fixed in (9.2.30) (or η_{12} in (9.2.31)) we must keep the ratio s_{12}/s_{34} fixed as both $\to\infty$.

This corresponds to the single-Regge graph fig. 9.1(*c*). There are obviously three possible single-Regge limits of the amplitude depending on whether we take s_{34}, s_{45} or $s_{35}\to\infty$.

(*b*) *The double-Regge limit.* Here z_1, $z_2\to\infty$, the other angle and the invariants in (9.2.32) being fixed. This means s_{12}, s_{34} and $s_{45}\to\infty$, t_1, t_2 fixed, and with the ratio $s_{12}/s_{34}s_{45}$ fixed to keep ω_{12} and η_{12} fixed.

This corresponds to the double-Regge graph fig. 9.1(*b*), but other double-Regge limits like fig. 9.1(*d*) can be obtained by permuting the final-state particles.

(*c*) *The helicity limit.* This has ω_{12} (and η_{12})$\to\infty$, with z_1, z_2, t_1 and t_2 all fixed, so $s_{12}\to\infty$ with s_{34}, s_{45}, t_1, t_2 fixed. Since this involves $\cos\omega_{12}\to\infty$ it is clearly not a physical limit.

Obviously (*a*) is just the same as the single-Regge limit in $2\to2$

scattering except that one of the final-state 'particles' is actually a two-particle state with fixed invariant mass. It is thus similar to resonance production in quasi-two-body processes and requires little further discussion. But (b) and (c) are quite new, and depend in an essential way on there being three particles available in the final state. They will be considered below.

This discussion can readily be generalized to any multi-particle final state. In the single-Regge limit those invariants which overlap the given Reggeon line (e.g. s_{12} and s_{34} in fig. 9.1 (c)) all tend to infinity, with fixed ratios, and all the other independent invariants (t_1, t_2, s_{45}) are held fixed. In the multi-Regge limit those invariants which overlap any Reggeon line (e.g. s_{12}, s_{34}, s_{45} in fig. 9.1 (b)) tend to infinity, and the others are held fixed. The ratios of those invariants which overlap a given Reggeon are held fixed, while those invariants which overlap several Reggeons (for example s_{12} overlaps α_1 and α_2 in fig. 9.1 (b)) tend to infinity like the products of the invariants of the individual lines (for example $s_{12} \sim s_{34}s_{45}$). In the helicity limit only those invariants which overlap two Reggeons tend to infinity, with a fixed ratio so that the Toller angle between those two Reggeons tends to infinity.

We shall now examine in more detail the Reggeization of the $2 \to 3$ amplitude, fig. 9.1. Since we are interested in using the results in the s-channel physical region, some authors have preferred to use the $O(2,1)$ group-theory method (whose application in $2 \to 2$ scattering was mentioned in section 6.6); see Bali, Chew and Pignotti (1967), Toller (1969), Jones, Low and Young (1971). However we shall use the Sommerfeld–Watson transform of the t-channel partial-wave series, and assume that this can be continued in the t's without difficulty.

In the single-Regge limit (a) we are concerned with the t-channel process $2 + \bar{3} \to (\bar{1}5) + 4$ where $(\bar{1}5)$ is a quasi-particle (see fig. 9.4 (a)). So following section 4.6 we begin with the t-channel partial-wave series (4.5.10)

$$\left.\begin{aligned} A(t_1, z_1; \omega_{12}; t_2, z_2) &= \sum_{J_1=0}^{\infty} \sum_{\lambda=-J_1}^{J_1} (2J_1+1)\, A_{J_1}(t_1; t_2, z_2)\, d^{J_1}_{0\lambda}(z_1)\, e^{i\lambda\omega_{12}} \\ &= \sum_{\lambda=-\infty}^{\infty} \sum_{J_1 \geqslant |\lambda|} (2J_1+1)\, A_{J_1}(t_1; t_2, z_2)\, d^{J_1}_{0\lambda}(z_1)\, e^{i\lambda\omega_{12}} \end{aligned}\right\} \tag{9.3.1}$$

where J_1 is the angular momentum of $\bar{3}$ with respect to 2, and in addition to summing over all partial waves we have also summed

over all the possible helicities λ for the quasi-particle $(\bar{1}5)$. By angular-momentum conservation $|\lambda|$ cannot be greater than J_1. (Remember that for simplicity we are assuming that all the particles $1, \ldots, 5$ are spinless.) The second expression in (9.3.1) seems more appropriate for continuing in J_1 (though in fact it may be better to continue in λ first: see Goddard and White (1971), White (1971, 1973*b*)). The factor $e^{i\lambda\omega_{12}}$ appears because (see (4.4.7) and (4.2.14)) ω_{12} gives the azimuthal angle in the 'decay' $(\bar{1}5) \to \bar{1} + 5$, and by definition λ is measured in the direction of motion of $(\bar{1}5)$.

We then replace the sum in (9.3.1) by the Sommerfeld–Watson integral (4.6.1) in the complex J_1 plane, and draw back the integration contour to expose the leading Regge pole $\alpha_1(t_1)$ whose contribution can be written

$$A^{\mathrm{R}}(t_1, z_1; \omega_{12}; t_2, z_2) = \Gamma(-\alpha_1(t_1))\, \gamma_1(t_1)\, (z_1)^{\alpha_1(t_1)} \sum_{\lambda=-\infty}^{\infty} e^{i\lambda\omega_{12}} \gamma_\lambda(t_1; t_2, z_2) \tag{9.3.2}$$

where we have factorized the residue into a part $\gamma_1(t_1)$ for the 2–$\bar{3}$ vertex, and $\gamma_\lambda(t_1; t_2, z_2)$ for the $(\bar{1}5)$–4 vertex, and have included the nonsense factor $\Gamma(-\alpha)$. If we define

$$\beta(t_1, \omega_{12}; t_2, z_2) = \sum_{\lambda=-\infty}^{\infty} e^{i\lambda\omega_{12}} \gamma_\lambda(t_1; t_2, z_2) \tag{9.3.3}$$

the Fourier transform of γ_λ, and take the asymptotic form

$$(z_1)^{\alpha_1} \sim (s_{34})^{\alpha_1},$$

we can rewrite this more conveniently as

$$A^{\mathrm{R}}(s_{12}, s_{34}, s_{45}, t_1, t_2) = \Gamma(-\alpha_1(t_1))\, \gamma_1(t_1)\, \beta(t_1, \omega_{12}; t_2, z_2)\, (s_{34})^{\alpha_1} \tag{9.3.4}$$

just like the $2 \to 2$ case (6.8.1).

For the double-Regge limit we start from a double partial-wave decomposition in z_1 and z_2 (Ter-Martirosyan 1965, Kibble 1963), i.e.

$$A(t_1, z_1; \omega_{12}; t_2, z_2) = \sum_{J_1, J_2=0}^{\infty} \sum_{\lambda} (2J_1+1)\,(2J_2+1) \times A_{J_1 J_2 \lambda}(t_1, t_2)\, d^{J_1}_{0\lambda}(z_1)\, d^{J_2}_{\lambda 0}(z_2)\, e^{i\lambda\omega_{12}} \tag{9.3.5}$$

where $|\lambda| \leqslant J_1, J_2$. Then if we make the Sommerfeld–Watson transform in both J's and expose the leading Reggeon in each channel, we get in the double-Regge asymptotic limit

$$A^{\mathrm{R}}(s_{12}, s_{34}, s_{45}, t_1, t_2) = \Gamma(-\alpha_1(t_1))\, \gamma_1(t_1)\, (s_{34})^{\alpha_1(t_1)} \times \beta(t_1, \eta_{12}, t_2)\, \Gamma(-\alpha_2(t_2))\, \gamma_2(t_2)\, (s_{45})^{\alpha_2(t_2} \tag{9.3.6}$$

where $\beta(t_1, \eta_{12}, t_2)$ is the coupling at the central vertex $(\alpha_1 \alpha_2 4)$ and depends on the Toller angle as well as the t's.

Apart, perhaps, from the inclusion of the η_{12} dependence these results are just what one would naïvely expect from drawing diagrams like fig. 9.1 (b). However, we have certainly not done full justice to the problem because we have not bothered much about the discontinuities in the different invariants, and in particular we have completely ignored the fact that Reggeons have signature and hence have discontinuities for both positive and negative s, which give the amplitude its phase. We must now remedy this.

The assumption that there are no simultaneous Regge discontinuities in overlapping-channel invariants means that for example the discontinuity in s_{34} must not itself have a discontinuity in s_{45}, though it may have one in s_{12}. So we expect that the s_{34} discontinuity may involve terms like

$$(-s_{34})^{\alpha_1-\alpha_2}(-s_{12})^{\alpha_2} V_2(\eta_{12}) + (-s_{34})^{\alpha_1-\alpha_2}(s_{12})^{\alpha_2} V_2'(\eta_{12}) \qquad (9.3.7)$$

where the V's are real functions of the η's (for negative t_1, t_2). Both terms $\sim |s_{34}|^{\alpha_1} |s_{45}|^{\alpha_2}$ since $s_{12} \sim s_{34} s_{45}$ in the double-Regge limit, but the first term is cut for positive s_{12} as well as s_{34}, while the second is not. We also want the Reggeons to have a definite signature, so that for example the Reggeon α_1 gives a discontinuity for positive s_{34} and an equal one for negative s_{34} (up to a $\pm$ sign depending on its signature $\mathscr{S}_1$) and so we have equal amplitudes under the interchange $2 \leftrightarrow 3$. There are thus four different terms, from fig. 9.8, and combining them, in the physical region where all the Regge functions are real, gives (Drummond, Landshoff and Zakrzewski 1969b)

$$A^{\mathrm{R}}(s_{12}, s_{34}, s_{45}, t_1, t_2) = \Gamma(-\alpha_1(t_1))\, \gamma_1(t_1)\, (s_{34})^{\alpha_1(t_1)}\, \Gamma(-\alpha_2(t_2))$$
$$\times \gamma_2(t_2)\, (s_{45})^{\alpha_2(t_2)} [\xi_1 \xi_{21} (\eta_{12})^{\alpha_1(t_1)} V_1(t_1, t_2, \eta_{12}) + \xi_2 \xi_{12} (\eta_{12})^{\alpha_2(t_2)} V_2(t_1, t_2, \eta_{12})] \qquad (9.3.8)$$

where
$$\xi_i = \mathrm{e}^{-\mathrm{i}\pi\alpha_i} + \mathscr{S}_i, \quad \xi_{ij} = \mathrm{e}^{-\mathrm{i}\pi(\alpha_i - \alpha_j)} + \mathscr{S}_i \mathscr{S}_j \qquad (9.3.9)$$

This may be re-expressed more conveniently as

$$A^{\mathrm{R}}(s_{12}, s_{34}, s_{45}, t_1, t_2) = \gamma_1(t_1)\, R_1(t_1, s_{34})$$
$$\times G_{12}^4(t_1, t_2, \eta_{12})\, R_2(t_2, s_{45})\, \gamma_2(t_2) \qquad (9.3.10)$$

where
$$R_i(t_i, s) \equiv \xi_i(t_i)\, \Gamma(-\alpha_i(t_i))\, s^{\alpha_i(t_i)} \qquad (9.3.11)$$

and
$$G_{ij}^4(t_i, t_j, \eta_{ij}) \equiv \xi_i^{-1} \xi_{ji} (\eta_{ij})^{\alpha_i(t_i)}$$
$$\times V_1(t_i, t_j, \eta_{ij}) + \xi_j^{-1} \xi_{ij} (\eta_{ij})^{\alpha_j(t_j)} V_2(t_i, t_j, \eta_{ij}) \qquad (9.3.12)$$

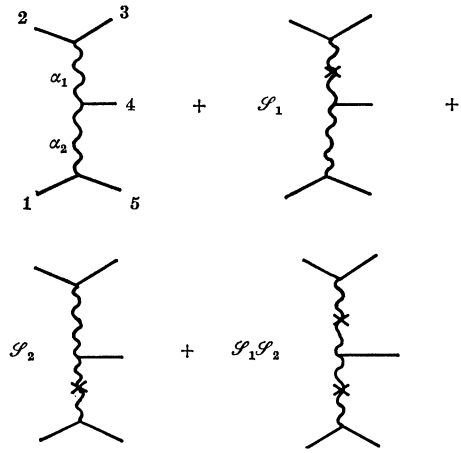

FIG. 9.8 The four different terms in the double-Regge amplitude stemming from the signature properties of the Reggeons. The × implies that the Reggeon is twisted ($s \to -s$) like the twisted ladders of fig. 8.11.

We can regard (9.3.11) as the Reggeon propagator, and all the phase complexity has been put into G^4_{12}, the coupling of particle 4 to the two Reggeons.

For more complicated amplitudes with extended chains of Reggeons like fig. 9.6 (a) we simply increase the number of propagators and G's in the obvious manner. However, with six lines a new type of configuration with a triple-Reggeon coupling, fig. 9.6 (b) becomes possible. In this case we can write (Landshoff and Zakrzewski 1969)

$$A^{\mathrm{R}} = \gamma(t_1)\, R_1(t_1, s_{345})\, \gamma(t_2)\, R_2(t_2, s_{456})\, \gamma(t_3) \times R_3(t_3, s_{234})\, G_{123}(t_1, t_2, t_3, \eta_{12}, \eta_{23}, \eta_{31}) \quad (9.3.13)$$

where again all the phase problems are contained in G_{123}. A careful analysis (de Tar and Weis 1971) finds

$$G_{123}(t_1, t_2, t_3, \eta_{12}, \eta_{23}, \eta_{31}) = \xi_3^{-1}\xi_{312}\overline{V}_{12} + \xi_1^{-1}\xi_{123}\overline{V}_{23} + \xi_2^{-1}\xi_{231}\overline{V}_{31} + \xi_1^{-1}\xi_2^{-1}\xi_3^{-1}\, \mathrm{e}^{-\mathrm{i}\pi(\alpha_1+\alpha_2+\alpha_3)}(1 + \mathscr{S}_1\, \mathrm{e}^{\mathrm{i}\pi\alpha_1} + \mathscr{S}_2\, \mathrm{e}^{\mathrm{i}\pi\alpha_2} + \mathscr{S}_3\, \mathrm{e}^{\mathrm{i}\pi\alpha_3})\overline{V}_{123}$$

where

$$\left.\begin{aligned} \overline{V}_{ij} &= (\eta_{ki})^{\alpha_i}(\eta_{jk})^{\alpha_j} V_{ij} \\ \overline{V}_{ijk} &= (\eta_{ij})^{\frac{1}{2}(\alpha_i+\alpha_j-\alpha_k)}(\eta_{jk})^{\frac{1}{2}(\alpha_j+\alpha_k-\alpha_i)}(\eta_{ki})^{\frac{1}{2}(\alpha_k+\alpha_i-\alpha_j)} V_{ijk} \\ \xi_{ijk} &\equiv \mathrm{e}^{-\mathrm{i}\pi(\alpha_i-\alpha_j-\alpha_k)} + \mathscr{S}_i\mathscr{S}_j\mathscr{S}_k \end{aligned}\right\} \quad (9.3.14)$$

and the V's are real functions. Any multi-Regge diagram can be expressed in terms of γ_i, R_i, G_{ij} and G_{ijk} as functions of the appropriate invariants (Weis 1973, 1974).

The other limit to be discussed is the helicity limit (*c*) (see Brower *et al.* 1973*b*). Starting from the double partial-wave series (9.3.5)

$$A(t_1,z_1;\omega_{12};t_2,z_2)=\sum_{\lambda=-\infty}^{\infty}\sum_{J_1=|\lambda|}^{\infty}\sum_{J_2=|\lambda|}^{\infty}(2J_1+1)(2J_2+1)\times A_{J_1J_2\lambda}(t_1,t_2)\,d^{J_1}_{0\lambda}(z_1)\,d^{J_2}_{\lambda 0}(z_2)\,\mathrm{e}^{\mathrm{i}\lambda\omega_{12}} \quad (9.3.15)$$

we express all three summations as contour integrals like (4.6.1)

$$A(t_1,z_1;\omega_{12};t_2,z_2)=\left(-\frac{1}{2\mathrm{i}}\right)^3\int\mathrm{d}\lambda\int\mathrm{d}J_1\int\mathrm{d}J_2\,\frac{(2J_1+1)(2J_2+1)A_{J_1J_2\lambda}(t_1,t_2)}{\sin(\pi\lambda)\sin(\pi(J_1-\lambda))\sin(\pi(J_2-\lambda))}\times d^{J_1}_{0\lambda}(-z_1)\,d^{J_2}_{\lambda 0}(-z_2)\,\mathrm{e}^{\mathrm{i}\lambda\omega_{12}} \quad (9.3.16)$$

which gives, from the Regge poles in J_1 and J_2, taking the asymptotic form of the $d^{\alpha_i}(-z_i)$ (even though we shall not in fact be making the z_i large),

$$A^{\mathrm{R}}(t_1,z_1;\omega_{12};t_2,z_2)=-\frac{1}{2\mathrm{i}}\int\mathrm{d}\lambda(-s_{34})^{\alpha_1(t_1)}(-s_{45})^{\alpha_2(t_2)}\times\frac{\mathrm{e}^{\mathrm{i}\lambda\omega_{12}}}{\sin\pi\lambda}\,\Gamma(\lambda-\alpha_1)\Gamma(\lambda-\alpha_2)\,\beta_\lambda(t_1,t_2)\,\gamma_1(t_1)\,\gamma_2(t_2) \quad (9.3.17)$$

where β_λ is the central coupling. Then using the fact that

$$\cos\omega_{12}=\tfrac{1}{2}(\mathrm{e}^{\mathrm{i}\omega_{12}}+\mathrm{e}^{-\mathrm{i}\omega_{12}})\sim\eta_{12}$$

we can rewrite this as

$$\begin{aligned}A^{\mathrm{R}}(t_1,z_1;\omega_{12};t_2,z_2)&=\frac{1}{2\pi\mathrm{i}}\int\mathrm{d}\lambda(-s_{34})^{\alpha_1}(-s_{45})^{\alpha_2}(-\eta_{12})^{\lambda}\,\Gamma(\lambda-\alpha_1)\Gamma(\lambda-\alpha_2)\,\Gamma(-\lambda)\times\beta_\lambda(t_1,t_2)\,\gamma_1(t_1)\,\gamma_2(t_2)\\&=\frac{1}{2\pi\mathrm{i}}\int\mathrm{d}\lambda(-s_{34})^{\alpha_1-\lambda}(-s_{45})^{\alpha_2-\lambda}(-s_{12})^{\lambda}\,\Gamma(\lambda-\alpha_1)\,\Gamma(\lambda-\alpha_2)\times\Gamma(-\lambda)\,\beta_\lambda(t_1,t_2)\,\gamma_1(t_1)\,\gamma_2(t_2)\end{aligned} \quad (9.3.18)$$

(see White (1972*a*), Brower *et al.* (1974) for details). Then for $s_{12}\to\infty$, s_{34}, s_{45}, t_1, t_2 fixed we find, on opening the λ contour, that the leading asymptotic behaviour stems from the 'helicity poles' of the Γ-functions at $\lambda=\alpha_i$, and gives terms

$$A^{\mathrm{R}}\sim(s_{12})^{\alpha_1}\quad\text{and}\quad\sim(s_{12})^{\alpha_2}$$

So in this helicity limit the Regge behaviour arises from the nonsense Γ-factors which relate the coupling of each Reggeon to the helicity of the other Reggeon.

We shall find that this limit is useful in the next chapter, but for multi-Regge analysis it is of course the various multi-Regge limits which concern us.

9.4 Multi-particle dual models*

In chapter 7 we introduced the idea of duality: that the Regge poles in the t channel already include the resonance poles in the s channel, at least in some average sense, and so it is a mistake to try to add these two types of contributions. The Veneziano model like (7.4.4), which we shall here take to be

$$V(s,t) = g\frac{\Gamma(-\alpha(s))\,\Gamma(-\alpha(t))}{\Gamma(-\alpha(s)-\alpha(t))} \tag{9.4.1}$$

gives a specific, though not unique, realization of this property, with Regge behaviour both in s at fixed t, and in t at fixed s. We now want to discuss the generalization of this result for many-particle amplitudes (see Veneziano 1974*a*, Schwarz 1973, Mandelstam 1974). It seems clear that this must be possible because for example in fig. 9.4(*a*) we treated $(\overline{15})$ like a single particle, and if we choose a positive value of t_2 such that $\alpha_2(t_2) = n$, a right-signature integer, we have a physical, and presumably dual, $2 \to 2$ process.

First it should be noted that in $2 \to 2$ scattering there is a different dual amplitude for each planar ordering of the particles (see fig. 7.7) so that the $V(s,t)$ term is represented by fig. 9.9(*a*) for which $s \leftrightarrow t$ involves just a cyclic permutation of 1, 2, 3, 4. But since $s \leftrightarrow u$ requires a non-cyclic permutation there is also a $V(s,u)$ term, fig. 9.9(*b*), which must be added separately, as must $V(t,u)$. So generalizing this idea of planar duality we can expect that the set of diagrams, fig. 9.10, which all have the same cyclic ordering of particles $1,\ldots,5$ will be dual to each other, but that for example the diagrams of fig. 9. 11 will comprise a separate dual term. In all there are 12 inequivalent orderings of the particles and hence 12 dual terms. Secondly the two Reggeons $\alpha_1(t_1)$ and $\alpha_2(t_2)$ in fig. 9.10(*a*) depend on completely unrelated variables t_{23} and t_{15}, so it is rather obvious that they cannot be dual to each other. It is Reggeons in overlapping channels, like t_{23} and s_{34} which have particle 3 in common (see fig. 9.10(*a*), (*b*)), which will be dual to each other.

* This section may be omitted at first reading.

https://doi.org/10.1017/9781009403269.010 Published online by Cambridge University Press

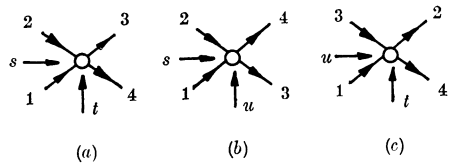

FIG. 9.9 The three inequivalent planar orderings of the particles which give the three terms in a $2 \to 2$ Veneziano amplitude like (7.4.17).

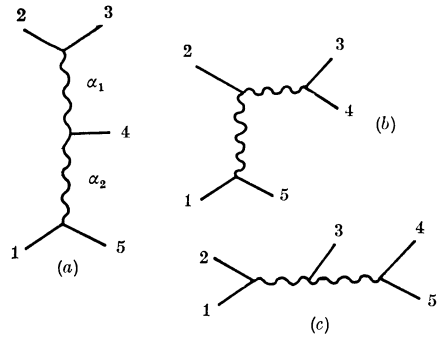

FIG. 9.10 Three different Reggeon amplitudes which involve the same planar cyclic ordering of particles $1, \ldots, 5$ and so should be represented by a single dual amplitude.

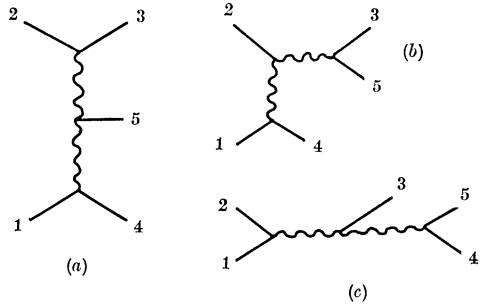

FIG. 9.11 Some Reggeon amplitudes which are dual to each other, but not to those in fig. 9.10.

To extend (9.4.1) we begin by rewriting it as

$$V(s,t) = gB_4(-\alpha(s), -\alpha(t)) \equiv g\int_0^1 \mathrm{d}x\, x^{-\alpha(s)-1}(1-x)^{-\alpha(t)-1} \tag{9.4.2}$$

where B_4 is known as the Euler β-function (see Veneziano (1968), Magnus and Oberhettinger (1949) p. 4). This integral is only defined

for $\alpha(s), \alpha(t) < 0$. As say $\alpha(s) \to 0$ we have

$$B_4(-\alpha(s), -\alpha(t)) \to \int_0^1 \mathrm{d}x\, x^{-\alpha(s)-1} + (\text{terms finite at } \alpha(s) = 0)$$
$$= -\frac{1}{\alpha(s)} + \text{finite terms} \tag{9.4.3}$$

so the pole at $\alpha(s) = 0$ arises from the divergence of the integrand at $x = 0$. We can continue past this singularity by integrating by parts, giving

$$B_4(-\alpha(s), -\alpha(t)) = \frac{\alpha(t)+1}{\alpha(s)} \int_0^1 \mathrm{d}x\, x^{-\alpha(s)}(1-x)^{-\alpha(t)-2} \tag{9.4.4}$$

which exhibits the pole at $\alpha(s) = 0$ and is defined for $\alpha(s) < 1$ where of course there is another pole of B_4. By repeating this process we find a sequence of poles at $\alpha(s) = 0, 1, 2, \ldots$. They can be obtained directly by expanding the integrand in the form

$$(1-x)^{-\alpha(t)-1} = \sum_{n=0}^{\infty} P_n(-\alpha(t))\, x^n \tag{9.4.5}$$

where $$P_n(-\alpha) \equiv \frac{(-1)^n}{n!}(-\alpha-1)(-\alpha-2)\ldots(-\alpha-n)$$

and integrating each term to give

$$B_4(-\alpha(s), -\alpha(t)) = \sum_{n=0}^{\infty} \frac{P_n(-\alpha(t))}{\alpha(s)-n} \tag{9.4.6}$$

So with a linear trajectory $\alpha(t)$ the residue of the pole at $\alpha(s) = n$ is a polynomial in t (and hence z_s) of degree n (cf. (7.4.13)).

The symmetry of (9.4.2) in $\alpha(s)$ and $\alpha(t)$ ensures that the channels s and t, which are related by a cyclic reordering of the particles $1, \ldots, 4$, have identical poles; but the poles in t arise from the other end of the range of integration at $x \to 1$, so that simultaneous poles in s and t are avoided. It is thus helpful to rewrite (9.4.2) as

$$V(s_{12}, t_{23}) = g \int_0^1 \mathrm{d}x_{12}\, \mathrm{d}x_{23} (x_{12})^{-\alpha(s_{12})-1} (x_{23})^{-\alpha(t_{23})-1} \delta(x_{12} + x_{23} - 1) \tag{9.4.7}$$

where we have associated an x variable with each channel which contains a pole (which arises for $x \to 0$), but by including the δ function have ensured that the overlapping s_{12} and t_{23} channels do not have simultaneous poles. It is also possible to insert an arbitrary function $f(x_{12}, x_{23})$ into the integrand of (9.4.7), analytic in $0 \leqslant x \leqslant 1$, in which case expanding f in a power series in the x's would give a sequence of Veneziano satellite terms like (7.4.15).

For the five-particle amplitude, fig. 9.10, we write similarly (Bardakci and Ruegg 1968, Virasoro 1969)

$$V(s_{12}, s_{34}, s_{45}, t_{23}, t_{15}) = gB_5(-\alpha(s_{12}), -\alpha(s_{34}), -\alpha(s_{45}), -\alpha(t_{23}), -\alpha(t_{15}))$$
$$\equiv g\int_0^1 \mathrm{d}x_{12}\,\mathrm{d}x_{34}\,\mathrm{d}x_{45}\,\mathrm{d}x_{23}\,\mathrm{d}x_{15}(x_{12})^{-\alpha(s_{12})-1}\ldots(x_{15})^{-\alpha(t_{15})-1}f(x_{12},\ldots,x_{15}) \tag{9.4.8}$$

which has poles for each of the possible pairings of external particles (in this planar configuration). The function f must be chosen so as to prevent simultaneous poles in overlapping channels like, for example, s_{34}, t_{23} and s_{45}, so it must not be possible for x_{34} and x_{23} or x_{45} to vanish simultaneously. So we require f to vanish unless

$$\left.\begin{aligned} x_{34} &= 1-x_{23}x_{45} && a\\ x_{45} &= 1-x_{34}x_{15} && b\\ x_{15} &= 1-x_{45}x_{12} && c\\ x_{12} &= 1-x_{15}x_{23} && d\\ x_{23} &= 1-x_{12}x_{34} && e \end{aligned}\right\} \tag{9.4.9}$$

This gives five equations for five unknowns but they are not all independent equations, and in fact two of the variables remain free. These can conveniently be taken to be x_{23} and x_{15}. Then d gives x_{12} in terms of these, and e and a give

$$x_{34} = \frac{1-x_{23}}{1-x_{15}x_{23}}, \quad x_{45} = \frac{1-x_{15}}{1-x_{15}x_{23}}$$

respectively; equations b and c are consistent with these results. So we can write from a, b and e

$$f(x_{12},\ldots,x_{15}) = \delta(1-x_{34}-x_{23}x_{45})\,\delta(1-x_{45}-x_{34}x_{15})\,\delta(1-x_{23}-x_{12}x_{34}) \tag{9.4.10}$$

We could also multiply by any analytic function of the x's to give satellite terms. These δ-functions can be used to perform the integrations over x_{34}, x_{45} and x_{23} giving

$$B_5(-\alpha(s_{12}), -\alpha(s_{34}), -\alpha(s_{45}), -\alpha(t_{23}), -\alpha(t_{15}))$$
$$= \int_0^1 \mathrm{d}x_{23}\,\mathrm{d}x_{15}(1-x_{15}x_{23})^{-\alpha(s_{12})-1}\left(\frac{1-x_{23}}{1-x_{15}x_{23}}\right)^{-\alpha(s_{34})-1}$$
$$\times\left(\frac{1-x_{15}}{1-x_{15}x_{23}}\right)^{-\alpha(s_{45})-1}(x_{23})^{-\alpha(t_{23})-1}(x_{15})^{-\alpha(t_{15})-1}(1-x_{15}x_{23})^{-1} \tag{9.4.11}$$

or

$$B_5(-\alpha(s_{12})-\alpha(s_{34}),-\alpha(s_{45}),-\alpha(t_{23}),-\alpha(t_{15}))=\int_0^1 \mathrm{d}x_{23}\,\mathrm{d}x_{15}$$
$$\times (x_{23})^{-\alpha(t_{23})-1}(x_{15})^{-\alpha(t_{15})-1}(1-x_{23})^{-\alpha(s_{34})-1}(1-x_{15})^{-\alpha(s_{45})-1}$$
$$\times (1-x_{15}x_{23})^{-\alpha(s_{12})+\alpha(s_{45})+\alpha(s_{34})} \qquad (9.4.12)$$

The complete five-particle dual amplitude is the sum of 12 terms like (9.4.12) involving different planar orderings of the five external particles. These are necessary to give the Reggeons signature since, for example, the signature properties of $\alpha(t_{23})$ and $\alpha(t_{15})$ require the four diagrams of fig. 9.8.

To examine the poles of this amplitude we put

$$-\alpha(s_{12})+\alpha(s_{45})+\alpha(s_{34})\equiv -\beta \qquad (9.4.13)$$

and expand
$$(1-x_{15}x_{23})^{-\beta}=\sum_{n=0}^{\infty}(x_{15}x_{23})^n P_n(-\beta) \qquad (9.4.14)$$

and integrate term-by-term to obtain (Hopkinson and Plahte 1968)

$$B_5=\sum_{n=0}^{\infty}P_n(-\beta)\int_0^1 \mathrm{d}x_{23}\,\mathrm{d}x_{15}(x_{23})^{-\alpha(t_{23})-1+n}(x_{15})^{-\alpha(t_{15})-1+n}$$
$$\times (1-x_{23})^{-\alpha(s_{34})-1}(1-x_{15})^{-\alpha(s_{45})-1}$$
$$=\sum_{n=0}^{\infty}P_n(-\beta)\,B_4(-\alpha(t_{23})+n,-\alpha(s_{34}))$$
$$\times B_4(-\alpha(t_{15})+n,-\alpha(s_{45})) \qquad (9.4.15)$$

Then if we expand the first B_4 as in (9.4.6)

$$B_5=\sum_{m=0}^{\infty}\frac{1}{-\alpha(t_{23})+m}\sum_{n=0}^{m}P_n(-\beta)\,P_{m-n}(-\alpha(_{34}))$$
$$\times B_4(-\alpha(t_{15})+n,-\alpha(s_{45}))$$

giving a residue of the pole at $\alpha(t_{23})=m$ of degree m in s_{34}, the angular variable for the t_{23} channel, so we have a daughter sequence of spins $k=0,\ldots,m$. The residue contains the four-point Veneziano formula for $(2\bar{3})+\bar{4}\to\bar{1}+5$ as one would expect from factorization in fig. 9.10(*a*). However, while the highest trajectory contains just single resonances at $\alpha(t_{23})=m$, all the daughter trajectories are multiply degenerate (Fubini and Veneziano 1969, Fubini, Gordon and Veneziano 1969), so simple amplitude factorization does not hold except on the leading trajectory. By excluding Veneziano satellites we have kept the daughter spectrum as simple as possible (Gross 1969), but none the less there are a very large number of particles. In fact

for a given m the number of levels is given by the number of ways of choosing non-negative integers n_i which satisfy

$$n_1 + 2n_2 + 3n_3 + \ldots = m$$

For large m this increases as $e^{(2\pi/\sqrt{6})m}$. It is of course a moot point whether one should take this seriously as a prediction of the model or whether it simply stems from the fact that we are unrealistically trying to represent a continuous branch cut by a sequence of poles.

To obtain the double-Regge limit of (9.4.12) we make the replacements

$$\alpha(s) = \alpha^0 + \alpha' s \xrightarrow[s\to\infty]{} \alpha' s, \quad x_{23} \equiv \frac{y_{23}}{-s_{34}}, \quad x_{15} \equiv \frac{y_{15}}{-s_{45}}$$

so

$$(1-x_{23})^{-\alpha(s_{34})-1} \to \left(1+\frac{y_{23}}{s_{34}}\right)^{-\alpha' s_{34}} \to e^{-y_{23}\alpha'}$$

$$(1-x_{15})^{-\alpha(s_{45})-1} \to e^{-y_{25}\alpha'}$$

$$(1-x_{23}x_{15})^{-\alpha(s_{12})+\alpha(s_{34})+\alpha(s_{45})} \to e^{(-y_{23}y_{15}s_{12}/s_{35}s_{45})\alpha'}$$

and hence

$$B_5 \to (-s_{34})^{\alpha(t_{23})}(-s_{45})^{\alpha(t_{15})} \int_0^\infty dy_{23}\, dy_{15} (y_{23})^{-\alpha(t_{23})-1} (y_{15})^{-\alpha(t_{15})-1} \times e^{-(y_{23}+y_{15}+(y_{23}y_{15}s_{12}/s_{34}s_{45}))\alpha'} \quad (9.4.16)$$

This gives the double-Regge form (9.3.10) with an explicit form for the dependence on the Toller angle in V which can be shown to be (Drummond *et al.* 1969*a*)

$$V_1(t_1, t_2, \eta_{12}) = \frac{1}{\Gamma(-\alpha_1)\Gamma(-\alpha_2)} \sum_{n=0}^{\infty} \frac{\Gamma(-\alpha_1 - n)\Gamma(-\alpha_2 + \alpha_1 - n)}{n!(\eta_{12})^n} \quad (9.4.17)$$

and similarly for V_2 (where $t_1 = t_{23}$, $t_2 = t_{25}$, $\alpha_1 = \alpha(t_{23})$, $\alpha_2 = \alpha(t_{25})$).

To generalize (9.4.8) to an N-particle amplitude we write for a given cyclic labelling of the particles (Chan 1968, Koba and Nielson 1969)

$$V_N = gB_N = g \int_0^1 f(x) \prod_{m,\,n} (x_{mn})^{-\alpha_{mn}-1} dx_{mn} \quad (9.4.18)$$

and the full amplitude will be the sum of $\frac{1}{2}(N-1)!$ terms for all the inequivalent non-cyclic permutations of the particles. A given $\alpha_{mn} \equiv \alpha(s_{mn})$ is specified by the channel invariant

$$s_{mn} = (p_m + p_{m+1} + \ldots + p_n)^2 \quad (9.4.19)$$

as shown in fig. 9.12(*b*), and to prevent simultaneous poles occurring in overlapping channels we must insert into $f(x)$

$$\delta(x_{mn} + \prod_{k,\,l} x_{kl} - 1) \quad (9.4.20)$$

https://doi.org/10.1017/9781009403269.010 Published online by Cambridge University Press

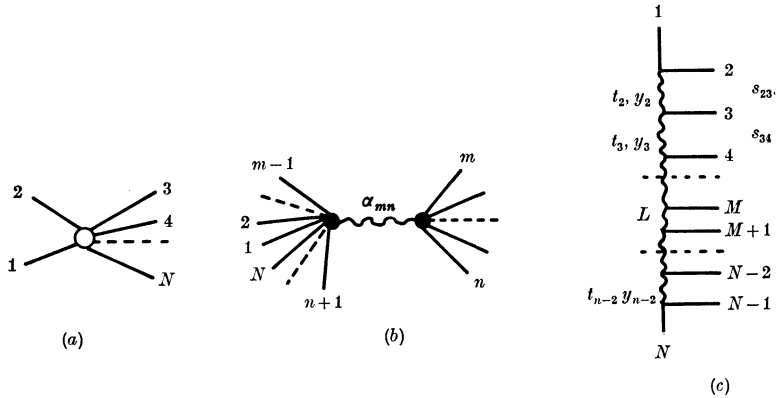

FIG. 9.12 (*a*) $1+2\to 3+\ldots+N$ amplitude with a cyclic ordering of the particles. (*b*) The α_{mn} trajectory exchange. (*c*) Labelling for $y_n = x_{1n}$.

where the kl are all the channels which overlap mn. To exhibit these we define $N-3$ variables

$$y_n \equiv x_{1n}, \quad n = 2, 3, \ldots, N-2 \tag{9.4.21}$$

as shown in fig. 9.12(*c*). Then all the other x's are related to these by (Chan and Tsou 1969)

$$x_{mn} = \frac{a_{m,n-1}\, a_{m-1,n}}{a_{m,n}\, a_{m-1,n-1}}, \quad 2 \leqslant m < n \leqslant N-1 \tag{9.4.22}$$

where

$$a_{mn} \equiv 1 - \prod_{k=m}^{n} y_k, \quad y_1 = y_{N-1} \equiv 0 \tag{9.4.23}$$

and it is found that the constraint (9.4.20) is incorporated by writing

$$B_N = \int_0^1 \mathrm{d}y_2 \ldots \mathrm{d}y_{N-2} \prod_{i=2}^{N-3} (1 - y_i y_{i+1})^{-1} \prod_{m,n} (x_{mn}(y))^{-\alpha_{mn}-1} \tag{9.4.24}$$

This agrees with the result (9.4.12) for $N = 5$, and the resulting multi-Regge behaviour corresponding to fig. 9.12(*c*) is

$$\begin{aligned} B_N \to\ & \Gamma(-\alpha(t_2))\,(-s_{23})^{\alpha(t_2)}\, V(t_2, t_3, \eta_{23})\, \Gamma(-\alpha(t_3))\,(-s_{34})^{\alpha(t_3)} \\ & \times V(t_3, t_4, \eta_{34}) \ldots \Gamma(-\alpha(t_{N-2}))\,(-s_{N-2,\,N-1})^{\alpha(t_{N-2})} \end{aligned} \tag{9.4.25}$$

where the V's are given by (9.4.17). This accords with (9.3.10) except that of course our single planar amplitude lacks the signature factors.

It is also possible to include internal symmetry in these multi-particle dual models. This is achieved by incorporating the quark ($q\bar{q}$) structure of the mesons, just as we did in section 7.5 (Chan and Paton 1969).

https://doi.org/10.1017/9781009403269.010 Published online by Cambridge University Press

Each meson is represented by a matrix, the rows corresponding to the quark index, and the columns to the anti-quark index. Thus if we consider just the isospin symmetry the quarks are the $I = \frac{1}{2}$ isodoublets (5.2.2), and a meson will be represented by a 2×2 matrix: a Kronecker $\delta_{\alpha\beta}$ if it is an isoscalar $I = 0$ (equation (5.2.7)), and the isospin Pauli matrices (5.2.5) $(\tau_i)_{\alpha\beta}$, $i = 1, 2, 3$ if it is the ith component of an isotriplet $I = 1$ (equation (5.2.8)). $I = 0$ and 1 are the only values which can be made from two $I = \frac{1}{2}$ quarks so there are no exotic states. It is convenient to introduce the notation $(\tau_0)_{\alpha\beta} = \delta_{\alpha\beta}$ so that the set τ_i, $i = 0, 1, 2, 3$, includes all four possible isospin states which a particle may have.

The Chan–Paton rule is that to include isospin in a B_N corresponding to a given cyclic ordering of the particles $1, \ldots, N$ we multiply it by a factor $\frac{1}{2}\operatorname{tr}(\tau_{i_1}, \tau_{i_2}, \tau_{i_3}, \ldots, \tau_{i_N})$ (where tr = trace). This factor has the same cyclic symmetry as that of B_N, and gives the correct $q\bar{q}$ structure with no exotics in any intermediate state. This can be seen by writing for the L exchange particle in fig. 9.12(*c*).

$$\tfrac{1}{2}\operatorname{tr}(\tau_{i_1} \ldots \tau_{i_N}) = \sum_{i_L=0}^{3} [\tfrac{1}{2}\operatorname{tr}(\tau_{i_1} \ldots \tau_{i_M} \tau_{i_L})][\tfrac{1}{2}\operatorname{tr}(\tau_{i_L} \tau_{iM+1} \ldots \tau_{i_N})] \tag{9.4.26}$$

which obviously has the desired factorization and isospin content for the residue of particle L, with exchange degeneracy between $I = 0$ and $I = 1$ particles. This can be extended from SU(2) to SU(3) simply by replacing the τ's by the λ matrices of table 5.1. But of course the method is only applicable in the limit of exact SU(3) degeneracy, which is far from the actual experimental situation.

In the last few years this dual formalism has undergone many developments which we shall not attempt to cover in any detail. The reader desiring to follow them can consult such excellent reviews as those of Veneziano (1974*a*), Schwarz (1973), Mandelstam (1974) and Scherk (1975).

We mentioned in section 3.3 that straight trajectories like those of the dual model are produced by a relativistic harmonic oscillator potential, and it has proved possible to re-express the dual model in an operator formalism in which particle states are created by an infinite set of harmonic oscillator creation operators a_μ^n, $n = 0, 1, \ldots, \infty$, operating on the basic vacuum state (Fubini *et al.* 1969, Fubini and Veneziano 1970, 1971). This makes it much easier to discuss such features as the resonance spectrum, and in particular the degeneracy

of the daughters. But there is a fundamental problem that to ensure the Lorentz covariance of the theory the creation operators must be four-dimensional ($\mu = 0, 1, 2, 3$) and the inclusion of the time dimension produces so-called 'ghost' states, with negative residues, which would violate causality (see section 1.4). The same problem occurs in quantum electrodynamics where the creation of time-like photons would cause difficulties were it not for the fact that the Lorentz gauge condition ensures that such states are eliminated (Bjorken and Drell 1965). This is possible because the massless nature of the photon means that there can be no longitudinal photons either (the helicity $\lambda = \pm 1$ only, not 0), so the longitudinal and time-like components can be arranged to cancel.

It has been found that likewise in dual models, if $\alpha(0) = 1$ for the leading trajectory, then an infinite set of gauge conditions can be imposed which eliminates all the ghosts. In fact this is true for up to 26 space–time dimensions. But of course such a restriction is very unphysical and makes it quite impossible to regard the model as a prototype for real physics even in the meromorphic limit. It does mean, however, that the resulting dual field theory is closely related to other field theories with massless particles, in particular to quantum electrodynamics with massless photons and electrons, to the Yang–Mills field theory, and to quantum gravity with a massless spin = 2 graviton. In fact these field theores can be obtained as limits of dual field theory when the trajectory slope $\alpha' \to 0$ (see Veneziano 1974).

A further development has been to visualize this operator formalism as describing the motion of a quantized massless relativistic string (Goddard *et al.* 1973, Mandelstam 1973, Scherk 1975). A meson may be thought of as a string with free ends moving under internal tension counter-balanced by the centrifugal force due to its rotation (fig. 9.13). The maximum angular momentum for a given energy ($\equiv$ mass) occurs when the string is rigid, as in fig. 9.13 (a), and simply rotates, while lower-angular-momentum states of the same energy occur if there are also vibrational modes (like those of a violin string) whose frequencies will be multiples of the fundamental rotation frequency. This produces the daughter spectrum at a given mass. Internal symmetry can be incorporated by imagining the string to have quarks tied to its ends.

The motion of the string will in time trace out a world sheet like a twisted ribbon (fig. 9.13 (c)) and the gauge conditions correspond to the requirement that only vibrations perpendicular to this world sheet

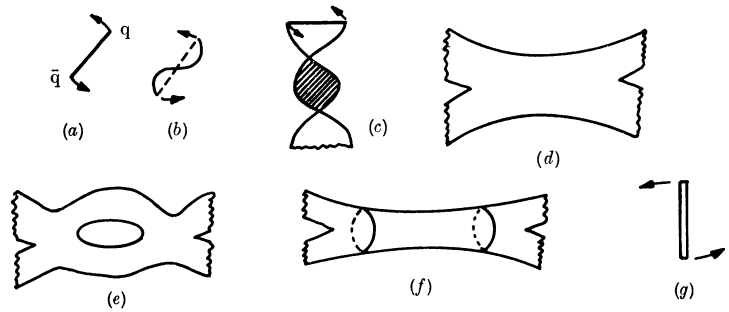

FIG. 9.13 (*a*) A rotating string with quarks at its ends. (*b*) A vibrational mode of the string. (*c*) World sheet of a rotating string. (*d*) String–string scattering. (*e*) Re-normalization loop in string–string scattering. (*f*) A tube corresponding to the Pomeron. (*g*) Highest angular-momentum state for a closed string.

occur. A consistent unitary quantum theory of such a string is possible only if $\alpha(0) = 1$ and the dimensionality of space–time is $D = 26$.

One can picture the interactions of such strings as in fig. 9.13(*d*), which looks very like the duality diagram of fig. 7.7(*a*) (see Olive 1974). To unitarize the theory one must of course be able to include loops like fig. 9.13(*e*), but such loops give infinite contributions which are not susceptible to the usual renormalization techniques of standard field theory because of the infinite number of intermediate states available. However, there is also another type of loop, namely a tube (fig. 9.13(*f*)), which is the world sheet of a closed string. The maximum angular momentum of such a closed string, for a given energy, occurs when it is pulled rigid as in fig. 9.13(*g*), and it has twice the angular momentum of the corresponding open string, so $\alpha(0) = 2$. In fact it can be shown that

$$\alpha_{\text{tube}} = 2 + \frac{\alpha'}{2} t$$

where α' is the slope of the open-string trajectory. Since the closed string has no ends it can carry no quarks, and so has vacuum quantum numbers, and it has therefore been identified with the Pomeron. The fact that the intercept is at 2 rather than 1 is another embarrassment, but perhaps if the intercept of the ordinary Reggeons could be brought down to $\alpha(0) = \frac{1}{2}$ then the Pomeron would come down to 1 as well. In the zero-slope limit the Pomeron field theory reduces to that of a graviton.

This dual field theory could be the first hint of a fundamental theory of strong interactions in which dual Reggeons play the central role. However, the fact that at present the theory seems to be restricted

to integer trajectory intercepts, high space–time dimensionality (D can be reduced from 26 to 10 in some versions), and is not readily renormalizable, makes it necessary to reserve judgement, and we shall not pursue the theory further here.

9.5 Multi-Regge phenomenology

Because the number of independent variables increases so rapidly with the number of particles ($= (3N-10)$ for an N-particle amplitude) many-particle processes have been much less well explored than those with two particles in the final state ($N = 4$). Thus to examine thoroughly the $2\to 3$ amplitude we need, ideally, sufficient events to map the probability distribution in five different variables, or four at a given incident energy. Further, since the double-Regge region requires s_{12}, s_{34}, $s_{45}\to\infty$ with $s_{12}/s_{34}s_{45}$ fixed, to get both s_{34} and s_{45} large enough we need a very large s_{12}. But at such large s_{12} the given three-body final state will be found in only a small fraction of the events. For this reason it has become more usual to try and analyse many-body reactions 'inclusively' as we shall describe in the next chapter, rather than concentrating on a particular final state exclusively. Nevertheless, it is important to discover what Regge theory has to say about individual many-body processes.

We shall concentrate on $2\to 3$ scattering as in fig. 9.1. From (1.8.5) the double differential cross-section, integrated over t_{23}, t_{15} at fixed s_{12}, will be (see (1.8.17))

$$\frac{\mathrm{d}^2\sigma}{\mathrm{d}s_{34}\,\mathrm{d}s_{45}}(s_{12},s_{34},s_{45}) = \frac{1}{2\lambda^{\frac{1}{2}}(s,m_1^2,m_2^2)}\int\prod_{i=3}^{5}\left(\frac{\mathrm{d}^3p_i}{2p_{i0}(2\pi)^3}\right)$$
$$\times(2\pi)^4\,\delta^4(p_1+p_2-p_3-p_4-p_5)\,\delta(s_{34}-(p_3+p_4)^2)$$
$$\times\,\delta(s_{45}-(p_4+p_5)^2)\,|A(1+2\to 3+4+5)|^2 \qquad (9.5.1)$$

which gives the distribution of events in the Dalitz plot, fig. 9.2, as a function of s_{34} and s_{45} for a given s_{12}. (If the particles have spin a sum over the helicities of A_H is implied as usual – see (4.2.5).)

The single-Regge limits like fig. 9.1 (c) are characterized by a fixed small value of one of these invariants, say s_{45}, with $s_{34}\sim s_{12}\to\infty$, and so there are three single-Regge regions as shown in fig. 9.14 (a). For example in $\pi^+\mathrm{p}\to\pi^+\pi^0\mathrm{p}$ we may have $\pi^+\mathrm{p}\to(\pi^0\pi^+)\,\mathrm{p}$, $\pi^+\mathrm{p}\to\pi^0(\pi^+\mathrm{p})$ and $\pi^+\mathrm{p}\to\pi^+(\pi^0\mathrm{p})$. Particular examples where two of the final-state particles are correlated as resonances, such as $(\pi^0\pi^+)=\rho^+$ or

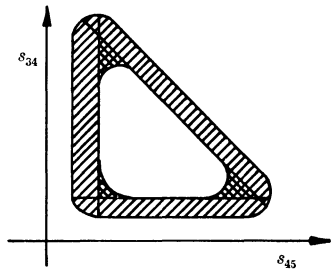

(*a*)

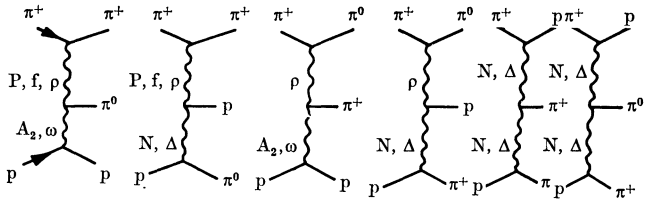

(*b*)

FIG. 9.14 (*a*) Dalitz plot for large s_{12} showing the three single-Regge regions (hatched) and the three double-Regge regions (cross-hatched). (*b*) Double-Regge exchange diagrams for $\pi^+p \to \pi^+\pi^0 p$.

$(\pi^+p) = \Delta^{++}$, give quasi-two-body reactions of the type already discussed in chapter 6, and in fact single-Regge analysis is identical to that for two-body final states except for the dependence on $s_{45} = m_{45}^2$, the invariant mass, and the (45) 'decay' angular distribution.

Of greater interest are the various double-Regge limits, like fig. 9.1(*b*) which requires s_{12}, s_{34}, $s_{45} \to \infty$, $\eta_{12} = s_{12}/s_{34}s_{45}$ fixed. Now from (9.2.30) η_{12} is related to ω_{12}, and since ω_{12} is a physical angle it is restricted to $\cos\omega_{12} \geqslant -1$ which gives (after some manipulation, see Chan *et al.* (1967))

$$(\sqrt{-t_{23}} + \sqrt{-t_{15}})^2 + m_4^2 \geqslant \frac{s_{34}s_{45}}{s_{12}} = \frac{1}{\eta_{12}} \tag{9.5.2}$$

Now Regge theory is applicable only when the interaction is peripheral, and we expect that the amplitudes will be negligible for large values of t. Empirically this stems partly from the exponential t dependence of Regge couplings and partly from Regge shrinkage, but it is also necessary on theoretical grounds that $s \gg t$ for each Reggeon. Hence we must have $|t_{23}|$, $|t_{15}|$ small (i.e. $\not\gg 1\,\text{GeV}^2$), which means that $1/\eta_{12}$ in (9.5.2) is restricted to similar small values. So the three double-

https://doi.org/10.1017/9781009403269.010 Published online by Cambridge University Press

Regge regions are near the corners of the Dalitz plot (as in fig. 9.14(*a*)) where the products $s_{34}s_{45}$ etc. are not too big in view of the given fixed large s_{12}, though both s_{34} and s_{45} must be large enough to be in their respective Regge regions, i.e. $s_{34}, s_{45} \gg 1\,\mathrm{GeV}^2$. This 'cornering' effect stems just from the kinematics of peripheral interactions, and is not a verification of multi-Regge theory as such.

The six double-Regge exchange graphs for $\pi^+\mathrm{p} \to \pi^+\pi^0\mathrm{p}$ are shown in fig. 9.14(*b*).

To proceed further it is more or less essential to place some restrictions on the Regge parameters because fits to the data with all these diagrams and all the variable parameters which might reasonably be put into (9.3.10) would be too time-consuming. One way of doing this is to invoke the dual model. Of course, it is necessary to smooth out the poles to obtain Regge behaviour on the real axis. Also one must eliminate P exchange since the Pomeron does not appear in simple dual models.

Examples of such analyses are those of Peterson and Tornqvist (1969) on $\mathrm{K}^-\mathrm{p} \to \pi^0\pi^+\Lambda$ and related processes, chosen because no P exchange can occur, and those of Chan *et al.* (1970) who examined $\mathrm{K}^+\mathrm{p} \to \mathrm{K}^0\pi^+\mathrm{p}$, $\mathrm{K}^-\mathrm{p} \to \overline{\mathrm{K}}_0\pi^-\mathrm{p}$, and $\pi^-\mathrm{p} \to \mathrm{K}^0\mathrm{K}^-\mathrm{p}$. The allowed planar diagrams are shown in fig. 9.15, and using them good agreement with the data was obtained. On inserting the known trajectory functions there remains just one free parameter, the overall normalization. See Berger (1971*a*) for a more complete survey.

A more simple version with many of the same features is the Chan–Loskiewicz–Allison (1968) model in which one writes, labelling the particles as in fig. 9.12(*c*) for convenience,

$$A_N = \prod_{i=2}^{N-2} (G_i s_i + F_i)\,(s_i+1)^{\alpha_i^0 - 1}\,(\mathrm{e}^a s_i + 1)^{\alpha' t_i} \qquad (9.5.3)$$

where

$$s_i \equiv s_{i\,i+1} \equiv (p_i + p_{i+1})^2, \quad t_i = [p_1 - (p_2 + p_3 + \ldots + p_i)]^2 \qquad (9.5.4)$$

This has the property that for all $s_i \gg 1$ it gives the multi-Regge form

$$A_N \sim \prod_{i=2}^{N-2} G_i (s_i)^{\alpha_i^0}\,\mathrm{e}^{(a + \log s_i)\alpha' t_i} \qquad (9.5.5)$$

like (9.3.6), but it neglects all the Toller-angle and spin effects at the vertices. For $s_i \to 0$ the ith term $\to F_i$ a constant, which provides a very crude parameterization of low sub-energy effects (which in fact provide the bulk of the events) but without the resonance structure which is

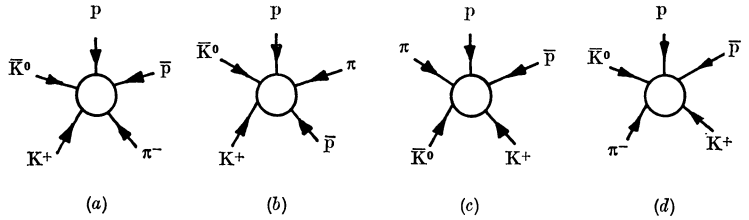

FIG. 9.15 Different orderings for the process $K^+p \to K^0\pi^+p$ (all particles drawn ingoing) with no exotic pairings. These are all the planar diagrams allowed by duality, but (*d*) is an illegal duality diagram because the λ quark would have to cross from $\bar{K}^0$ to K^+.

necessary for a really good description of the data. The full amplitude is a sum of terms like A_N for all inequivalent permutations of the particles. Though not good enough for detailed quantitative work this parameterization provides a manageable approximation with many of the desired qualitative features. Plahte and Roberts (1969) have produced an improved version.

The conclusions of this chapter may be summarized as follows. A consistent multi-Regge theory seems to be possible, though at present to derive it one has to make unproven if plausible assumptions about the singularity structure which determines the Regge asymptotic behaviour. A dual model with such a multi-Regge structure can be constructed, though the internally self-consistent factorizing version of the model bears at most a rather limited resemblance to nature. However, it might eventually lead to a fundamental theory of strong interactions. Phenomenologically multi-Regge theory can be tested only on that rather small fraction of the events for a given process which occur in the multi-Regge region of phase space. It appears to be satisfactory, and, despite their obvious limitations, dual models have enjoyed some phenomenological success. But many-particle amplitudes depend on too many variables for a really detailed comparison of theory and experiment to be made. Hence for example it has so far been possible to more or less ignore the Regge-cut corrections to the dominant pole exchanges.

It will be evident that a better way of analysing inelastic scattering processes is necessary, and this is provided by the Mueller–Regge approach to inclusive cross-sections, which is the subject of the next chapter.